

# The examination of graphene oxide for rechargeable lithium storage as a novel cathode material†

Cite this: *J. Mater. Chem. A*, 2013, **1**, 3607

Da-Wei Wang,<sup>ab</sup> Chenghua Sun,<sup>c</sup> Guangmin Zhou,<sup>d</sup> Feng Li,<sup>d</sup> Lei Wen,<sup>d</sup> Bogdan C. Donose,<sup>e</sup> Gao Qing (Max) Lu,<sup>a</sup> Hui-Ming Cheng<sup>\*d</sup> and Ian R. Gentle<sup>\*b</sup>

A sustainable cathode is critical to developing green lithium storage devices. Conducting polymers, radical polymers and carbonyl-based polymers are the three most important types of polymer-based sustainable cathode materials. Here we report that graphene oxide enriched with epoxide, without being reduced, is a promising sustainable carbonaceous cathode material for rechargeable lithium storage. Graphene oxide containing a large quantity of epoxide can have a high capacity of 360.4 mA h g<sup>-1</sup> at 50 mA g<sup>-1</sup>, which significantly surpasses those of many polymer cathodes and conventional lithium-transition metal oxide cathodes. The good stability of this epoxide-based cathode was demonstrated. Density functional theory calculations indicate that the lithiation of epoxide is energetically favorable (−1.21 eV) and the original epoxide structure can be restored after delithiation with a small barrier (0.23 eV).

Received 27th December 2012  
Accepted 18th January 2013

DOI: 10.1039/c3ta01658g

www.rsc.org/MaterialsA

## 1 Introduction

There is currently intense motivation to develop high specific energy batteries in large quantities for the electric/hybrid vehicle market and the electronics industry in general. The emerging large-scale usage of metal-based non-renewable cathode materials has raised the concern of material sustainability. The concept of “sustainable” or “green” lithium ion batteries was introduced by Tarascon, Armand, Chen and co-workers, and renewable organic cathodes have been recognized as an important family of this kind.<sup>1,2</sup> Sustainable carbonaceous materials can be produced in an eco-friendly way from biomass and exhibit robust surface chemistry favoring a wide range of applications.<sup>3</sup> However, only a few studies have considered the potential of carbonaceous materials as cathode materials for lithium batteries.<sup>4–7</sup> Reduced graphene oxide (rGO) is a two-dimensional oxygen-containing carbonaceous material. Its rich (electro) chemistry has inspired an increasing level of interest toward a

better understanding of the physicochemical behaviour of this two-dimensional material in energy storage applications. The interaction of rGO and its derivatives with lithium is of great potential importance for lithium storage. Along with the critical roles played by sheet thickness, defects and dopants,<sup>8–14</sup> lithiation of carbonyl/carboxyl functional groups on rGO is interesting and requires further study for a full understanding.<sup>4,6</sup>

Previous studies on the interaction between lithium ion and oxygen have focused solely on the carbon–oxygen double bond.<sup>2,4–7,15–20</sup> The carbon–oxygen double bonds in quinone-containing polymers (polyimide, poly(anthraquinonyl sulfide), Li<sub>2</sub>C<sub>6</sub>O<sub>6</sub>, etc.)<sup>2,15–20</sup> or carbonaceous nanostructures<sup>4–7</sup> interact with lithium ions in the following way: >C=O + Li<sup>+</sup> + e<sup>−</sup> ↔ >C–O–Li. The specific capacity of the carbonyl-based polymer cathodes is dependent on their molecular structure,<sup>16</sup> and can be subtly engineered through modifying the sulfur-connection position in poly(anthraquinonyl sulfide) cathodes.<sup>20</sup> These facts suggest that the interaction of lithium ions with oxygen attached to aromatic rings is sensitive to the nature of the oxygen functional group.

A theoretical calculation performed by Stournara *et al.* showed the high-potential lithiation of epoxide on GO, which suggests a new approach for use of GO as a cathode material in lithium storage.<sup>21</sup> The epoxide group () which has a carbon–oxygen single bond, could be very important for lithium storage on oxygen-containing carbon materials, but has been overlooked in previous studies. Epoxide is the most abundant functional group in GO and gives rise to distinct surface chemistry from that of rGO.<sup>22,23</sup> However, until now, whether epoxide-enriched GO can be electrochemically reactive to lithium ions is a fundamental yet unanswered question. In this work, the following questions are posed and tested: can epoxide react with lithium ions and, if so, how good is the lithiation

<sup>a</sup>Australian Research Council Centre of Excellence for Functional Nanomaterials, Australian Institute for Bioengineering and Nanotechnology, The University of Queensland, Brisbane, QLD 4072, Australia

<sup>b</sup>School of Chemistry and Molecular Biosciences, The University of Queensland, Brisbane, QLD 4072, Australia. E-mail: i.gentle@uq.edu.au

<sup>c</sup>Centre for Computational Molecular Science, Australian Institute for Bioengineering and Nanotechnology, The University of Queensland, Brisbane, QLD 4072, Australia

<sup>d</sup>Advanced Water Management Centre, The University of Queensland, Brisbane, QLD 4072, Australia

<sup>e</sup>Shenyang National Laboratory for Materials Science, Institute of Metal Research, Chinese Academy of Sciences, Shenyang, Liaoning 110016, P. R. China. E-mail: cheng@imr.ac.cn

† Electronic supplementary information (ESI) available: Computational methods and material characterization results: XPS, FTIR, XRD, Raman and cathode performance. See DOI: 10.1039/c3ta01658g

reactivity of epoxide? For the first time, we demonstrate that epoxide-enriched GO can be lithiated/de-lithiated as a rechargeable cathode with high capacity and good stability.

This study proceeded in two parts. Initially a sample of GO was prepared in a way intended to ensure that the epoxides were the major oxygen-containing functional surface groups, and the initial characterization and performance measurements were performed on that sample. The second part of the study involved samples of GO that were annealed at higher temperatures that had the effect of changing the proportion of surface groups so that epoxides were less dominant. This allowed us to determine the role of epoxide groups in lithiation of the surface.

## 2 Experimental

### 2.1 Synthesis and heat-deoxygenation of graphene oxide

A graphene oxide dispersion was prepared from graphite flakes as follows. Firstly 120 mL of concentrated  $\text{H}_2\text{SO}_4$  was slowly added to a ground powder mixture of expandable graphite flakes (1.0 g) and  $\text{KMnO}_4$  (6.0 g) at room temperature (25 °C) upon magnetic stirring. The green-colored solution was maintained at room temperature for 15 min and then transferred to a 50 °C bath for a continuous stirring of 5 hours. The color of the solution turned from dark green to purple, and finally to yellow. After cooling to room temperature, 10 mL of 30%  $\text{H}_2\text{O}_2$  together with 100 mL of water was poured into it. The reacted solution was centrifuged (4500 rpm for 30 min), and the supernatant was decanted away. The recovered colloidal graphite oxide (100 mg) was re-dispersed in neutral water (100 mL) by ultrasonic agitation for 2 hours and cryo-dried under vacuum. The thermal dehydration/deoxygenation of raw graphene oxide was conducted in an oven under ambient conditions. The heating temperatures were set as 100 °C, 130 °C, and 200 °C, and the duration was 2 hours for all temperatures. A slow ramp was applied at 2 °C  $\text{min}^{-1}$ . The annealed sample was cooled to room temperature naturally after heat-treatment.

### 2.2 Characterizations of the graphene oxide

X-ray powder diffraction was performed on a Bruker D8 Advance diffractometer. ATR-FTIR spectra were obtained on a Spectrum One spectrometer (Perkin Elmer). X-ray photoelectron spectroscopy (XPS) was performed using a Kratos Axis Ultra spectrometer with Al K $\alpha$  radiation (15 kV, 150 W). The high resolution C1s XPS spectra were recorded with a width of 14–20 eV, pass energy of 20 eV and an energy interval of 0.05 eV per step. The AFM image was collected using a WiTec Alpha 300 Raman/AFM Instrument (WiTec, Germany) operated in tapping mode, using SiNi triangular cantilevers (BudgetSensors, Bulgaria).

### 2.3 Electrochemical measurements of the graphene oxide

The electrochemical properties of GO cathodes in CR-2032 type coin cells were evaluated by a galvanostatic charge–discharge technique. The GO cathodes were prepared by mixing 70 wt% of an active material with 15 wt% conductive carbon black (super P) as a conducting agent and 15 wt% polyvinylidene fluoride dissolved in *N*-methyl-2-pyrrolidone as a binder to form a slurry,

which was then coated onto Al foil ( $d = 12$  mm), pressed and dried under vacuum at 80 °C for 12 h. The thickness of the active material layer is 20–25  $\mu\text{m}$ , while the mass of the active material on each cathode is estimated to be between 0.3 and 0.5 mg depending on the sample density. Coin cells were assembled in an argon-filled glove box with the samples as the working electrode, metallic lithium as the counter/reference electrode, a mixture of 1 M  $\text{LiPF}_6$  in ethylene carbonate, dimethyl carbonate and ethylmethyl carbonate (1 : 1 : 1 v/v) as the electrolyte. A Celgard 2400 polypropylene membrane was used as the separator. Charge–discharge measurements were carried out galvanostatically at various current densities over a voltage range of 1.50 to 4.50 V (vs.  $\text{Li}/\text{Li}^+$ ) using a battery testing system (LAND CT2001A). After the first discharge or the first recharge, the cells were disassembled in a glove box, and the working electrode was taken out and washed three times using a dimethyl carbonate solution. It was then transferred using a sealed container into the vacuum chamber of the XPS for surface analysis.

## 3 Results and discussion

The GO used in this work was exfoliated from graphite oxide. The crude GO was annealed at 100 °C for 2 hours to remove the adsorbed water (denoted as GO-100). Fig. 1 shows an atomic force microscopy image of stacked GO-100 sheets whose left edge is a monolayer (1.4 nm height) and right edge has four layers (5.6 nm height).<sup>24</sup> The chemical bonding of carbon with oxygen in GO-100 was analyzed using X-ray photoelectron spectroscopy (XPS), and it was found that GO-100 contains 69.0 at.% carbon and 31.0 at.% oxygen (Fig. S1 and Table S1<sup>†</sup>). The epoxide ( $\text{C}_2\text{O}$ ) group makes up the highest content (32.7 at.%) compared to the other oxygen functional groups (>C–OH, 0.93 at.%; >C=O, 3.40 at.%; O=C–OH, 3.35 at.%) that constitute the C 1s spectrum (Fig. 2a).

The electrochemical performance of the GO-100 cathode was tested in a CR-2032 type coin cell at increasing current densities (from 0.05 to 2 A  $\text{g}^{-1}$ ). At each current density the performance was measured over 5 cycles. The discharge–recharge curves are shown in Fig. 2b. Lithiation/delithiation of epoxide on the GO-100 cathode ranges over a broad potential, which is a pseudo-capacitive behaviour. The overall discharge capacity is 360.4 mA h  $\text{g}^{-1}$ , and the total recharge capacity is 385.8 mA h  $\text{g}^{-1}$  at 0.05 A  $\text{g}^{-1}$ . The discharge capacity at 0.1 A  $\text{g}^{-1}$  is 219.0 mA h  $\text{g}^{-1}$ , and nearly 90 mA h  $\text{g}^{-1}$  capacity can be preserved when the current density increases to 2 A  $\text{g}^{-1}$ . The surface  $\text{Li}^+$  storage acting on the epoxide on the GO-100 cathode rules out the need for ion diffusion into the bulk of electrode materials and hence results in high-rate performance. The coulombic efficiency is maintained close to 100% demonstrating that the GO-100 cathode is in fact rechargeable (Fig. S3<sup>†</sup>). It is interesting to note that graphite oxide has been studied as a cathode in primary lithium batteries as early as 1985 when its recharge ability was apparently not realised.<sup>25–28</sup> Following a 35-cycle rate test, the stability of a GO-100 cathode was subsequently examined at 0.1 A  $\text{g}^{-1}$  for another 60 cycles (Fig. 2c). The capacity remains at around 200 mA h  $\text{g}^{-1}$  during the successive cycles, demonstrating good

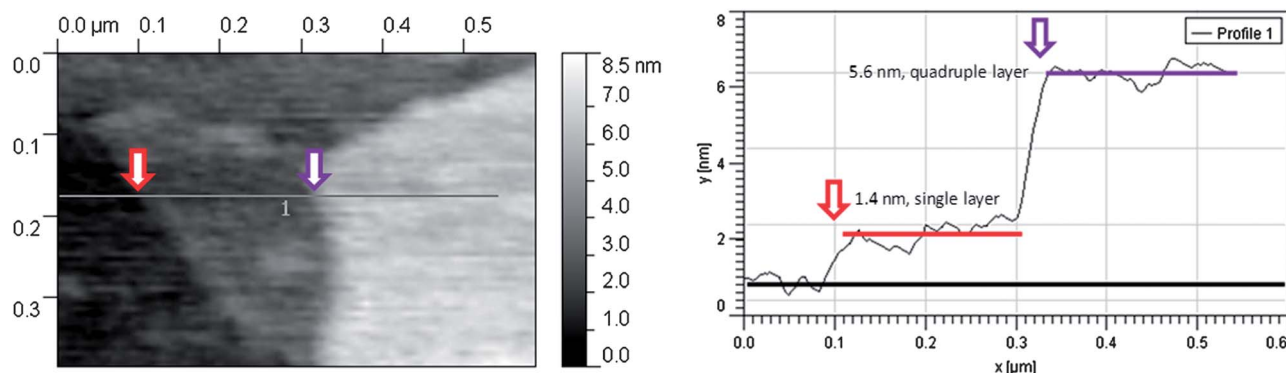


**Fig. 1** (Left) AFM topographical image of stacked GO nanosheets deposited on a Si substrate. (Right) Cross-section profile at different positions along the line in the left panel, revealing mono- and quadruple layer structures (generated by Gwyddion freeware software).

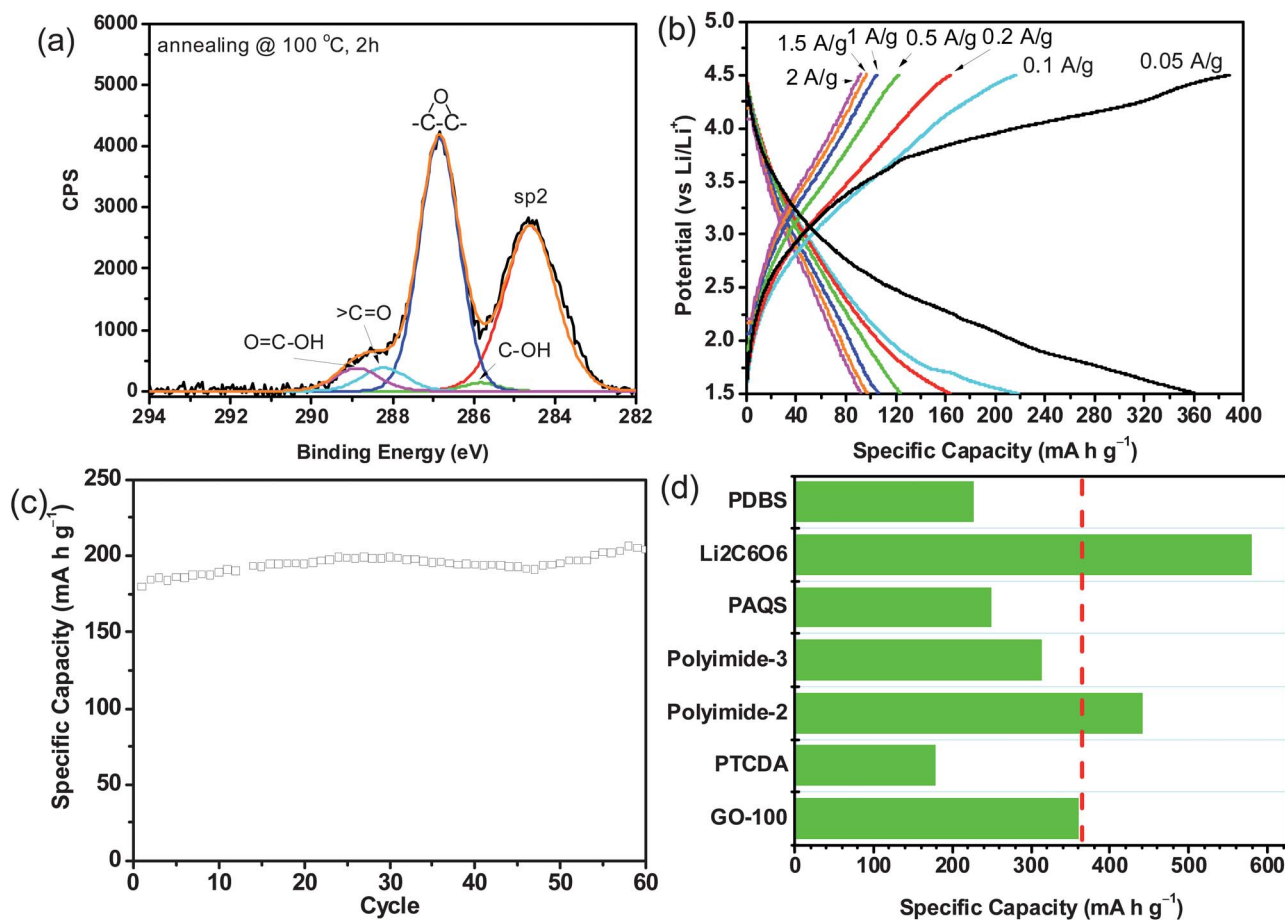


**Fig. 2** (a) High-resolution XPS C 1s spectrum of the GO-100 material (epoxide ( $\triangle$ ), hydroxyl ( $>C-OH$ ), carbonyl ( $>C=O$ ) and carboxyl ( $O=C-OH$ )). (b) The discharge/recharge potential–capacity profiles of a GO-100 cathode measured at different current densities. (c) The cycling stability of a GO-100 cathode measured at  $0.1 \text{ A g}^{-1}$ . (d) Comparison of the specific capacities of the epoxide-enriched GO-100 cathode with several carbonyl-based polymer cathodes: 3,4,9,10-perylene-tetracarboxylic acid-dianhydride (PTCDA),<sup>15</sup> polyimide-2/3,<sup>16</sup> poly(anthraquinonyl sulfide) (PAQS),<sup>19</sup>  $\text{Li}_2\text{C}_6\text{O}_6$ ,<sup>2</sup> and poly(2,5-dihydroxy-1,4-benzoquinonyl sulfide) (PDBS).<sup>18</sup>

stability of the epoxide-enriched GO cathode. It is worth noting that the lithiation capacity of the epoxide-enriched GO cathode outperforms those of many carbonyl-based polymer cathodes (Fig. 2d).<sup>2,15–19</sup> It is believed that the cathodic lithium storage on functionalized carbon nanostructures is due to the  $>C=O$  group in carbonyl or carboxyl groups.<sup>4–7</sup> However, the surface

oxygen functional groups on the GO-100 cathode are characteristic of epoxide, rather than carbonyl or carboxyl groups. Our results strongly suggest a new approach to store lithium through epoxide on GO cathodes, without reduction or deoxygenation. Note that the theoretical capacity of GO-100 could be as high as  $627.6 \text{ mA h g}^{-1}$  given that the oxygen content

(31.0 at.%) is in the form of epoxide groups and is fully reactive to lithium (provided that each epoxide stores one lithium ion). Although this is only a rough estimation, it is clear that graphene oxide shows great potential as an advanced metal-free cathode material.

To further clarify the role of epoxide in lithium storage, crude GO was annealed at 130 °C (labeled as GO-130) and 200 °C (labeled as GO-200) to selectively transform the surface oxygen-containing functional groups. Valence band spectroscopy (VBS) is a powerful tool to evaluate the change of oxygen functionalities on GO.<sup>22</sup> It is well known that the characteristic regions in the VB spectrum correspond to C 2p, C 2s and O 2s electrons, from lower binding energy to higher binding energy (Fig. 3a).<sup>22</sup> The GO-100 sample spectrum is dominated by O 2s with a peak centered at 26.9 eV and its Fermi edge at high energy (3.18 eV), revealing the insulating nature of the material (Fig. S4†). Thermal conversion gradually increases the contribution from C 2p states and simultaneously reduces the O 2s amounts, confirming that deoxygenation has taken place. Meanwhile, the Fermi edge shifts stepwise to lower binding energies indicating improved electron conduction from GO-130 (3.06 eV) to GO-200 (1.50 eV) (Fig. S4†). The changing nature of oxygen groups on the annealed GO cathodes was further confirmed by XPS

survey and high resolution O 1s spectra. The oxygen atomic concentration in GO-130 and GO-200 reduces to 29.1 at.% and 16.1 at.%, respectively (Fig. S4 and S5, Table S1†). Deconvolution of the O 1s spectrum for GO-130 reveals the enhanced contribution of hydroxyl accompanied by a reduction in epoxide concentration (Fig. 3b, Table S1†). Higher temperature annealing at 200 °C significantly decreases the contribution from all the oxygen moieties (Fig. 3c and Table S1†). Fourier transform infrared spectroscopy also confirms the component change of oxygen functional groups (Fig. S6†). X-ray diffraction profiles of the samples show the shift of the main peak towards higher angles, which is a sign of the gradual shrinkage of the intercalated compounds due to the loss of oxygen functional groups (Fig. S7†). Meanwhile, Raman spectra provide more information on the changes occurring in the sp<sup>2</sup> hybridized honeycomb lattice during oxygen removal as suggested by the increase of G-mode intensity and the shift of G-mode peak position (Fig. S8†).

The electrochemical performance of a GO-130 cathode and a GO-200 cathode was compared with that of a GO-100 cathode (Fig. S9†). All the cathodes exhibit similar pseudo-capacitive behavior. The discharge or charge specific capacities of GO-130 and GO-200 cathodes reduce dramatically when compared to GO-100. For instance, at 0.5 A g<sup>-1</sup>, the discharge capacity of the

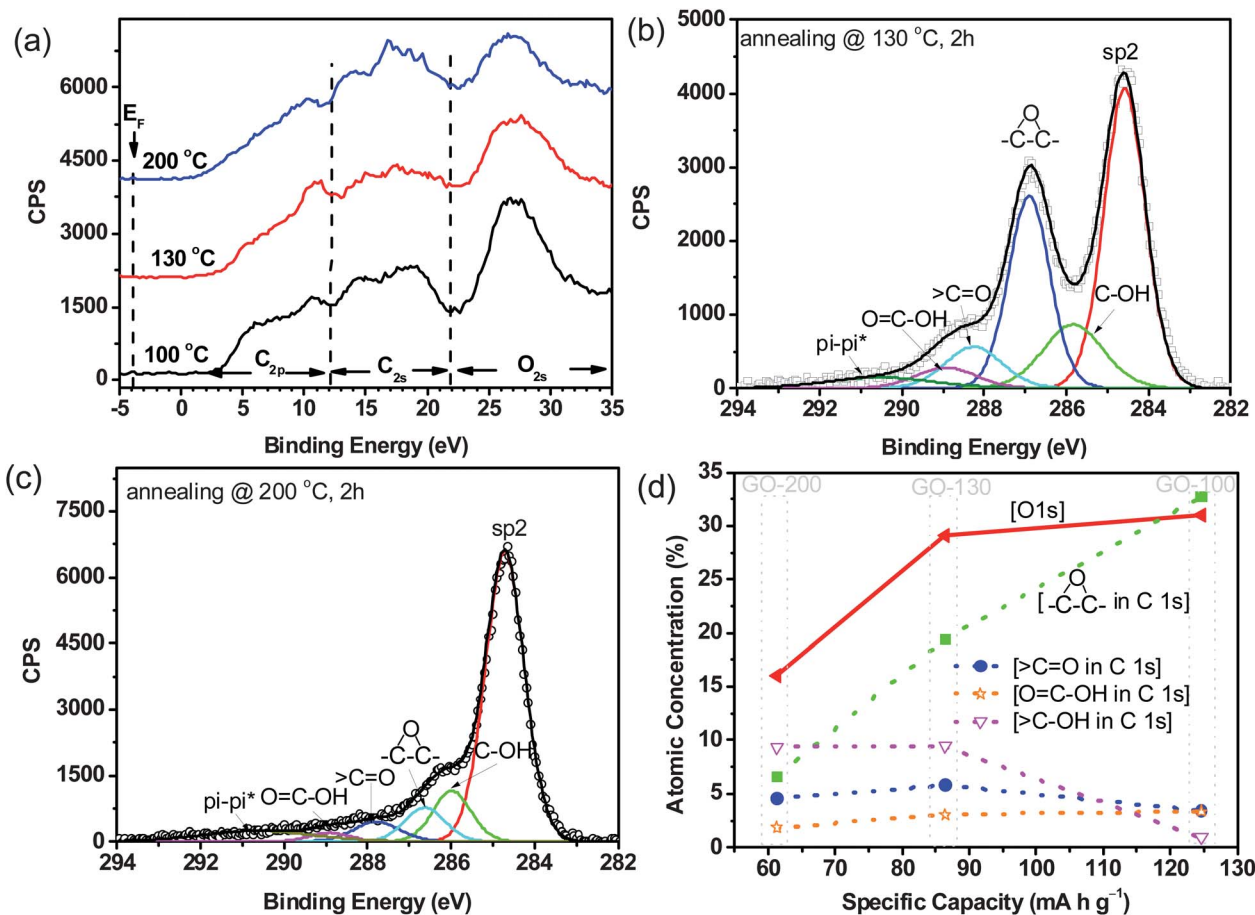


**Fig. 3** (a) VB spectra of GO cathodes annealed at 100 °C, 130 °C and 200 °C for 2 hours. XPS C 1s spectra of (b) GO-130 and (c) GO-200 cathodes. (d) The FTIR spectra of the GO-100, GO-130 and GO-200 cathodes. (d) Relationship between discharge capacity @ 0.5 A g<sup>-1</sup> and the atomic concentrations of O 1s and oxygen functional groups in C 1s (epoxide (◡◡), hydroxyl (>C-OH), carbonyl (>C=O) and carboxyl (O=C-OH)).

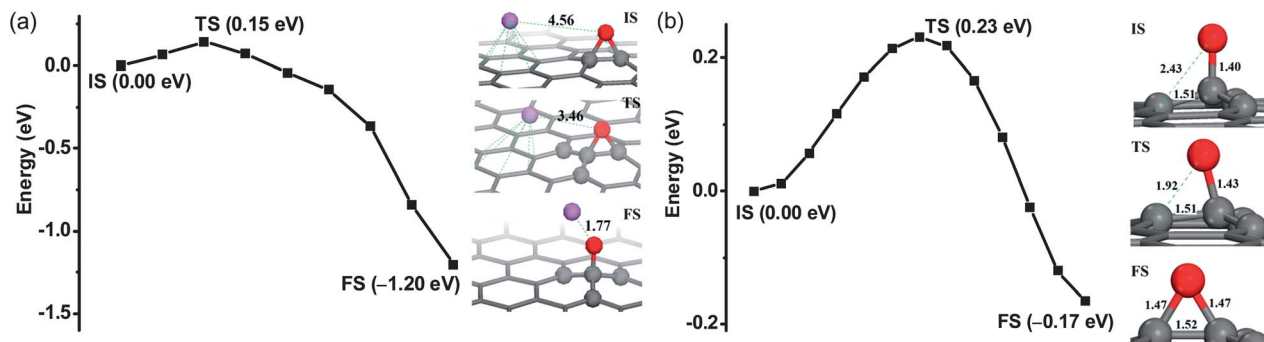


**Fig. 4** (a) Transformation intermediate states during the lithiation of  $\text{C}=\text{O}$ . (b) Transformation intermediate states from delithiated  $-\text{O}-\text{C}$  to  $\text{Li}-\text{O}-\text{C}$  (epoxide). Bond length and distance between atoms are in units of Å. Lithium: purple ball. Oxygen: red ball. Carbon: grey ball. X-Axis represents the reaction coordinate: IS: initial state, TS: transition state, and FS: final state.

GO-100 cathode is  $124.6 \text{ mA h g}^{-1}$ , while the corresponding capacities of the GO-130 and GO-200 cathodes are  $86.4$  and  $61.3 \text{ mA h g}^{-1}$ , respectively (Fig. S9a<sup>†</sup>). Substantial oxygen removal causes the extremely low capacity of the GO-200 cathode. The rate capability and cyclic stability of GO-130 are compared with those of GO-100 in Fig. S9b<sup>†</sup>. The discharge capacity of the GO-130 cathode at  $0.1 \text{ A g}^{-1}$  is  $120.3 \text{ mA h g}^{-1}$ , much less than that of the GO-100 cathode ( $218.3 \text{ mA h g}^{-1}$ ). As the current density gradually increases to  $1 \text{ A g}^{-1}$ , the capacity of the GO-130 cathode reduces to around  $70.2 \text{ mA h g}^{-1}$ . In stark contrast, the GO-100 cathode can deliver a capacity of  $92.0 \text{ mA h g}^{-1}$  even at  $2 \text{ A g}^{-1}$ . To determine the roles of oxygen functional groups in lithiation, the discharge capacities of the three cathodes are plotted against the atomic concentration of O 1s and carbon-oxygen bonds (epoxide, hydroxyl, carbonyl and carboxyl) that constitute the C 1s peak (Fig. 3d). It is evident that as the oxygen concentration increases the capacity is increased either. Considering that the atomic concentration of carbonyl and carboxyl stays nearly constant, this suggests that epoxide is responsible for this capacity increment because a large portion of the augmented oxygen species is epoxide. These results suggest that epoxide is related to the  $\text{Li}^+$  storage capacity, as an addition to the lithiation-active carboxyl and carbonyl.<sup>4-7</sup>

In order to better understand the origin of the lithiation activity of epoxide groups, the interaction of a lithium ion with an epoxide sitting on the graphene lattice was examined at the molecular level. Density functional theory (DFT) calculations were used to determine the nature of the lithiation of epoxide (Fig. 4). The reaction energy for epoxide lithiation is  $-1.21 \text{ eV}$ , which indicates that this reaction is energetically favorable. Moreover, as shown in Fig. 4a, the O atom in a Li-O cluster is linked to an aromatic lattice *via* a Li-O-C bond. When Li is removed from the Li-O-C bond, oxygen can restore the  $\text{C}=\text{O}$  structure after overcoming a small barrier ( $0.23 \text{ eV}$ ), suggesting that the lithium storage through epoxide is reversible, which is in agreement with the experimental results (Fig. 4b). To verify the DFT calculation results, we have recorded the oxygen group evolution on discharge and recharge by monitoring the *ex situ* XPS O 1s spectra for all the as-made, discharged and recharged GO-100 cathodes. The discharged and recharged GO-100 cathodes were recovered from the tested coin cells. Prior to Li uptake

the O 1s spectrum of the raw GO-100 cathode shows the components of C-O and C=O (Fig. S10<sup>†</sup>). Along with lithium storage the proportion of C-O reduces, while the content of Li-O sharply increases. As the removal of lithium during recharge proceeds, the intensity of the Li-O peak decreases accompanied by the increase of C-O, indicating that reversible lithiation of epoxide groups on the GO-100 cathode occurs.

## 4 Conclusions

The results of the electrochemical, spectroscopic and theoretical approaches suggest that epoxide groups on a GO cathode are lithiation reactive. The discharge capacity of the epoxide-enriched GO cathode can reach  $360.4 \text{ mA h g}^{-1}$  at  $0.05 \text{ A g}^{-1}$ , which is higher than that of many carbonyl-based cathodes.<sup>2,16-19</sup> Though a reaction path between lithium and epoxide is suggested, the validity of this mechanism needs to be verified by using more powerful *in operando* techniques. Nonetheless, we clearly demonstrate the excellent potential of epoxide-enriched graphene oxide as a rechargeable cathode for high-capacity lithium storage.

## Acknowledgements

The authors acknowledge the financial support from the University of Queensland (ECR009132, NSRSU600211 and Foundation Research Excellence Awards) and Australian Research Council Discovery Project (DP110100550). The authors also acknowledge the support from National Science Foundation of China (no. 50921004 and 51172242). Assistance from Dr Barry Wood for the XPS measurement is gratefully acknowledged. We also appreciate the generous grants of CPU time from both the University of Queensland and the Australian National Computational Infrastructure Facility. This work was performed in part at the Queensland node of the Australian National Fabrication Facility, a company established under the National Collaborative Research Infrastructure Strategy to provide nano- and microfabrication facilities for Australia's researchers. The authors acknowledge the facilities, and the scientific and technical assistance, of the Australian Microscopy & Microanalysis Research Facility at the Centre for Microscopy and Microanalysis, The University of Queensland.

## Notes and references

- 1 M. Armand, S. Grugeon, H. Vezin, S. Laruelle, P. Ribiere, P. Poizot and J. M. Tarascon, *Nat. Mater.*, 2009, **8**, 120–125.
- 2 H. Chen, M. Armand, G. Demailly, F. Dolhem, P. Poizot and J. M. Tarascon, *ChemSusChem*, 2008, **1**, 348–355.
- 3 M. M. Titirici and M. Antonietti, *Chem. Soc. Rev.*, 2010, **39**, 103–116.
- 4 H. R. Byon, B. M. Gallant, S. W. Lee and Y. Shao-Horn, *Adv. Funct. Mater.*, 2012, DOI: 10.1002/adfm.201200697.
- 5 S. W. Lee, B. M. Gallant, H. R. Byon, P. T. Hammond and Y. Shao-Horn, *Energy Environ. Sci.*, 2011, **4**, 1972–1985.
- 6 B. Z. Jang, C. G. Liu, D. Neff, Z. N. Yu, M. C. Wang, W. Xiong and A. Zhamu, *Nano Lett.*, 2011, **11**, 3785–3791.
- 7 S. W. Lee, N. Yabuuchi, B. M. Gallant, S. Chen, B. S. Kim, P. T. Hammond and Y. Shao-Horn, *Nat. Nanotechnol.*, 2010, **5**, 531–537.
- 8 E. Pollak, B. S. Geng, K. J. Jeon, I. T. Lucas, T. J. Richardson, F. Wang and R. Kostecki, *Nano Lett.*, 2010, **10**, 3386–3388.
- 9 E. Yoo, J. Kim, E. Hosono, H. Zhou, T. Kudo and I. Honma, *Nano Lett.*, 2008, **8**, 2277–2282.
- 10 X. F. Fan, W. T. Zheng and J. L. Kuo, *ACS Appl. Mater. Interfaces*, 2012, **4**, 2432–2438.
- 11 A. L. M. Reddy, A. Srivastava, S. R. Gowda, H. Gullapalli, M. Dubey and P. M. Ajayan, *ACS Nano*, 2010, **4**, 6337–6342.
- 12 Z. S. Wu, W. C. Ren, L. Xu, F. Li and H. M. Cheng, *ACS Nano*, 2011, **5**, 5463–5471.
- 13 D. Y. Pan, S. Wang, B. Zhao, M. H. Wu, H. J. Zhang, Y. Wang and Z. Jiao, *Chem. Mater.*, 2009, **21**, 3136–3142.
- 14 X. F. Li, D. S. Geng, Y. Zhang, X. B. Meng, R. Y. Li and X. L. Sun, *Electrochem. Commun.*, 2011, **13**, 822–825.
- 15 X. Y. Han, C. X. Chang, L. J. Yuan, T. L. Sun and J. T. Sun, *Adv. Mater.*, 2007, **19**, 1616–1621.
- 16 Z. P. Song, H. Zhan and Y. H. Zhou, *Angew. Chem., Int. Ed.*, 2010, **49**, 8444–8448.
- 17 Z. P. Song, T. Xu, M. L. Gordin, Y. B. Jiang, I. T. Bae, Q. F. Xiao, H. Zhan, J. Liu and D. H. Wang, *Nano Lett.*, 2012, **12**, 2205–2211.
- 18 K. Liu, J. M. Zheng, G. M. Zhong and Y. Yang, *J. Mater. Chem.*, 2011, **21**, 4125–4131.
- 19 Z. P. Song, H. Zhan and Y. H. Zhou, *Chem. Commun.*, 2009, 448–450.
- 20 W. Xu, A. Read, P. K. Koech, D. H. Hu, C. M. Wang, J. Xiao, A. B. Padmaperuma, G. L. Graff, J. Liu and J. G. Zhang, *J. Mater. Chem.*, 2012, **22**, 4032–4039.
- 21 M. E. Stournara and V. B. Shenoy, *J. Power Sources*, 2011, **196**, 5697–5703.
- 22 A. Ganguly, S. Sharma, P. Papakonstantinou and J. Hamilton, *J. Phys. Chem. C*, 2011, **115**, 17009–17019.
- 23 W. Gao, L. B. Alemany, L. J. Ci and P. M. Ajayan, *Nat. Chem.*, 2009, **1**, 403–408.
- 24 C. Gomez-Navarro, R. T. Weitz, A. M. Bittner, M. Scolari, A. Mews, M. Burghard and K. Kern, *Nano Lett.*, 2007, **7**, 3499–3503.
- 25 A. Hamwi and I. Alsaleh, *J. Power Sources*, 1994, **48**, 311–325.
- 26 P. Touzain, R. Yazami and J. Maire, *J. Power Sources*, 1985, **14**, 99–104.
- 27 R. Yazami and P. Touzain, *Synth. Met.*, 1985, **12**, 499–503.
- 28 M. Mermoux and P. H. Touzain, *J. Power Sources*, 1989, **26**, 529–534.